Biosensors and Bioelectronics 26 (2011) 2038–2044

Contents lists available at ScienceDirect

Biosensors and Bioelectronics

journal homepage: www.elsevier.com/locate/bios

The importance of interfacial design for the sensitivity of a label-free electrochemical immuno-biosensor for small organic molecules

Sook Mei Khor[a], Guozhen Liu[a], Callie Fairman[a], Sridhar G. Iyengar[b], J. Justin Gooding[a,*]

[a] School of Chemistry, The University of New South Wales, Sydney, NSW 2052, Australia
[b] AgaMatrix, Inc., 10 Manor Parkway, Salem, NH 03079, USA

ARTICLE INFO

Article history:
Received 30 June 2010
Received in revised form 27 August 2010
Accepted 31 August 2010
Available online 9 September 2010

Keywords:
Label-free electrochemical immuno-biosensor
Biotin
Small organic molecules
Interfacial design
Molecular wire
Oligo(ethylene glycol)

ABSTRACT

An immuno-biosensing interface comprising a mixed layer of an oligo(ethylene glycol) (OEG) component, and an oligo(phenylethynylene) molecular wire (MW) is described. The OEG controls the interaction of proteins and electroactive interferences with the surface and the MW allows electrochemical communication to the underlying glassy carbon electrode. The layers are formed from *in situ* generated-aryl diazonium cations. To the distal end of the MW, a redox probe 1,1′-di(aminomethyl)ferrocene is attached followed by the surface bound epitope (the structural feature the antibody selectively recognizes) to which an antibody would bind. Association or disassociation of the antibody with the sensing interface causes a modulation of the ferrocene electrochemistry. X-ray photoelectron spectroscopy, cyclic voltammetry, and square wave voltammetry have been used to characterize the step-wise fabrication of the sensing interface. The influence of the molar ratio of the MW and OEG deposited onto the sensor interface was explored relative to the final sensor sensitivity. Five combinations of MW/OEG 1:0, 1:20, 1:50, 1:75 and 1:100 were tested on sensor sensitivity detection for a model analyte (biotin) free in solution, via a displacement assay. The ratio of 1:50 was found to give the highest sensitivity. At this ratio, good reproducibility (RSD 6.8%) and repeatability (RSD 9.6%) was achieved. This immuno-biosensor provides an intervention free immuno-biosensing platform for agriculture and biomedical samples.

1. Introduction

The detection of small organic molecules (<1000 Da) (Guo et al., 2010) such as drugs and pesticides in biological, food and environmental samples is a continuing challenge in measurement science, especially with regard to on-site analysis performed by untrained personnel. Hence the development of an intervention free electrochemical immuno-biosensor for the specific detection of small organic molecules in complex samples is of great importance. One possible solution for detecting small organic molecules in complex matrices is the immuno-biosensing concept described recently by Liu et al. (2008). In this immuno-biosensing concept, a glassy carbon electrode is modified with a mixed layer of oligo(phenylethynylene) molecular wires (MWs) (Creager et al., 1999; Fan et al., 2001; Liu et al., 2007b; Viljas et al., 2008) and oligo(ethylene glycol) species (OEG) (Leckband et al., 1999; Liu and Gooding, 2006; McPherson et al., 1998; Zanini et al., 2007). To the end of the MW is attached a redox probe 1,1′-di(aminomethyl)ferrocene (FDMA), followed by an epitope (biotin) to which an antibody (monoclonal anti-biotin IgG antibody) is complexed. Complexation of the antibody immerses the redox probe in a protein environment and causes a significant attenuation of the current derived from the ferrocene moiety. The attenuation of current upon protein binding is attributed to the restriction of counter ions accessing the redox probe to balance the charge; thereby hindering the electron transfer (Fig. 1: Sensor 1). There is no labelling of antibody or antigen required and hence the device is used simply by placing it into a sample. When placed in a sample containing the target analyte (free biotin), transduction is achieved by antibody leaving the electrode surface due to the competition for the antibody between the surface bound epitope and the analyte. In other words, the current increases upon dissociation of the antibody from the surface bound epitope; an event motivated by the presence of the analyte in solution. This type of assay is referred to as a displacement assay (Fig. 1: Sensor 2). The dynamic range was reported to be between 30 ng mL^{-1} and 0.3 mg mL^{-1} with a lowest detected concentration of 30 ng mL^{-1} (Liu et al., 2008). As this assay relies on the relative affinity of the antibody for the surface bound epitope relative to the affinity for the target analyte in solution, the type of epitope (Bonanno and DeLouise, 2010), as well as the concentration of the epitope, the antibody and the target analyte (Rabbany et al., 1994) used are all important parameters in determining the sensitivity of the final immuno-biosensor.

* Corresponding author. Tel.: +61 2 9385 5384; fax: +61 2 9385 6141.
E-mail address: justin.gooding@unsw.edu.au (J.J. Gooding).

0956-5663/$ – see front matter © 2010 Elsevier B.V. All rights reserved.
doi:10.1016/j.bios.2010.08.082

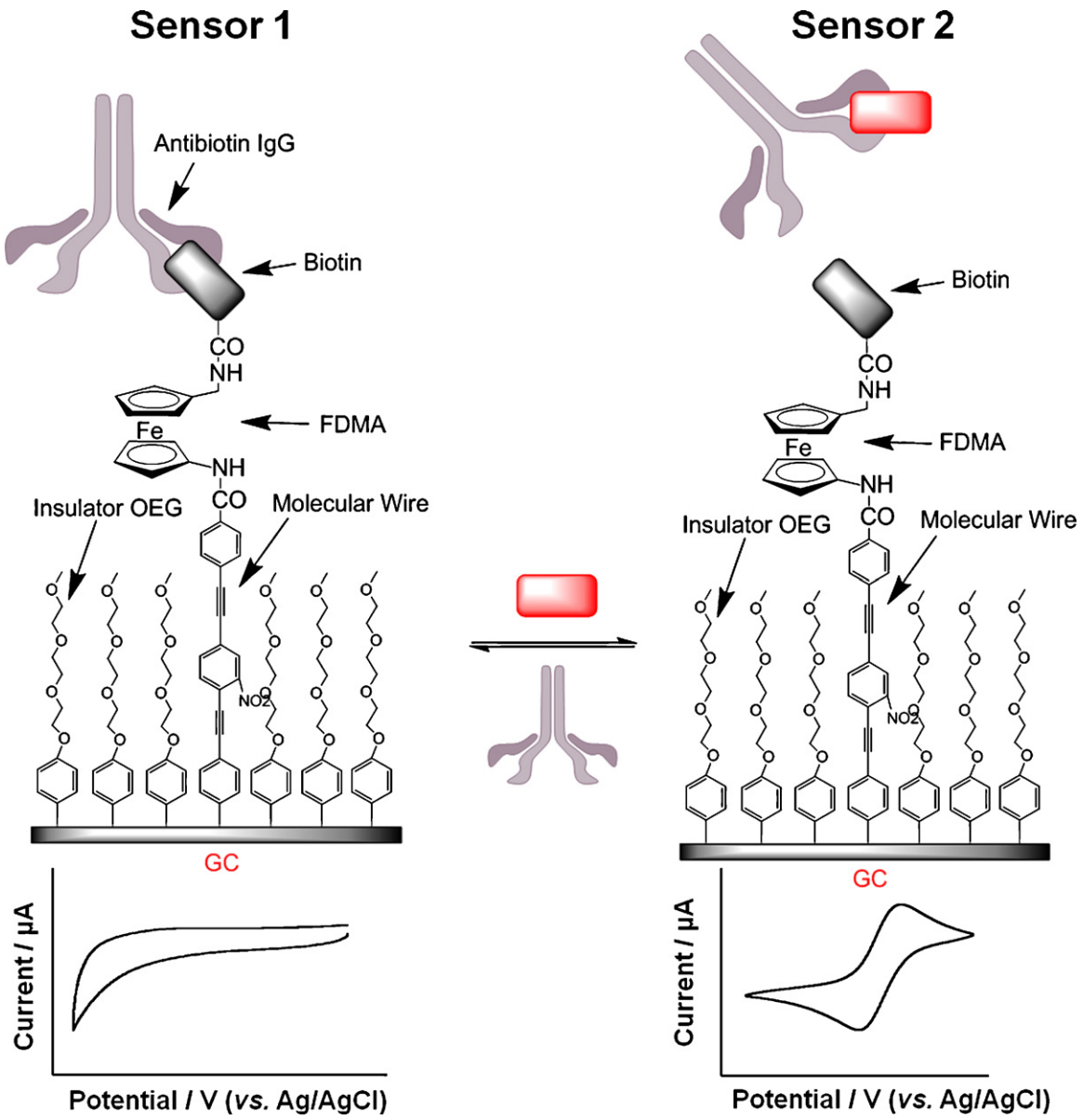

Fig. 1. Schematic of a label-free electrochemical immuno-biosensor. Sensor 1 shows the electrode surface before detection of the target analyte with the corresponding electrochemical signal. Note the antibody is not to scale, being many times larger than pictured. Sensor 2 shows the detection after the antibody is released with the expected increase in electrochemistry shown.

The sensitivity of this immuno-biosensor is also expected to be dependent on the interfacial design where an important variable will be the ratio of MW to insulator OEG (Fig. 1). The ratio of MW/OEG will influence the number of redox probe (FDMA) and epitope (biotin) which are bound to the electrode surface as well as the space available for specific antibody (monoclonal anti-biotin IgG antibody) to complex with the surface bound epitope (biotin). Hence the purpose of this paper is to report on the importance of interfacial design on sensor performance.

2. Experimental

2.1. Reagents and materials

The aryl diazonium cations used, OEG and MW were custom synthesized following procedures of Bahr et al. (2001) and Tour et al. (2001), respectively. The synthesis of the MW had been modified such that there was a carboxylic acid moiety at the distal end of the molecule. The FDMA was synthesized according to Ossola et al. (2003). 1,3-Dicyclohexylcarbodiimide (DCC), absolute ethanol, $NaNO_2$, monoclonal anti-biotin IgG antibody from goat, and biotin were obtained from Sigma–Aldrich. Sulfo-NHS–biotin was purchased from Pierce Chemical Company. Analytical grade K_2HPO_4, KH_2PO_4, KCl, NaOH, NaCl, $NaH_2PO_4{\cdot}2H_2O$, and HCl were purchased from Ajax Chemicals Pty. Ltd. All buffer solutions were prepared with Milli-Q^{TM} water with resistivity of 18.2 MΩ cm (Millipore, Sydney, Australia). Phosphate buffered saline (PBS) was made up by 0.137 M NaCl, 0.1 M $NaH_2PO_4{\cdot}2H_2O$, and adjusted to pH 7.4. Phosphate buffer was 0.05 M KCl, 0.05 M K_2HPO_4/KH_2PO_4, and adjusted to pH 7.0.

2.2. Electrode preparation for cyclic voltammetry (CV) and square wave voltammetry (SWV) measurements

All electrochemical measurements were performed with a BAS-100B/W electrochemical analyser (Bioanalytical Systems Inc.,

USA). Electrodes were a 3 mm diameter glassy carbon (GC) disk electrode (Bioanalytical Systems Inc., USA) used as the working electrode, a platinum flag (5 mm^2) as the counter and a Ag/AgCl (NaCl, 3 M) reference electrode, relative to which all potentials are quoted. GC electrodes were polished successively in 1.0, 0.3 and 0.05 μm alumina slurries (5 min each) of alumina in Milli-Q™ water on microcloth pads (Buehler, Lake Bluff, IL, USA). After each polishing the electrode was rinsed with Milli-Q™ water. Before derivatization, the GC electrodes were dried with an argon stream. For the displacement assay, the dissociation of the antibody from the surface bound epitope was monitored by SWV, measuring the current vs. potential profile (+0.8 V to 0 V) in the negative direction. For the SWV measurements, the parameters used were: step potential = 4 mV; frequency = 15 Hz; amplitude = 25 mV.

2.3. Construction of the label-free electrochemical immuno-biosensing interface

Aniline derivatives were converted to aryl diazonium cations (MW and OEG) by adding 1 mM of total corresponding amine (MW/OEG at different molar ratio of 1:0, 1:20, 1:50, 1:75, and 1:100) to a solution containing 2 mM $NaNO_2$ and 0.5 M HCl (Baranton and Belanger, 2005). The electrolyte solution was degassed with argon for at least 20 min prior to electrochemical modification. Surface derivatization of GC electrodes was conducted using CV with a scan rate of 100 mV s^{-1} for two cycles between +0.6 V and −1.1 V (Gooding, 2008; Liu et al., 2005, 2007a). The electrodes were rinsed with copious amounts of Milli-Q™ water and dried with argon prior to the next step of surface functionalization.

Covalent attachment of FDMA to carboxylic acid terminated mixed layer of MW/OEG was achieved by immersing the MW/OEG modified GC electrodes into an absolute ethanol solution containing 40 mM DCC and 5 mM FDMA overnight at 4 °C. Prior to the biotinylation process, the FDMA modified GC electrodes were rinsed with copious amounts of distilled ethanol followed by Milli-Q™ water, scanned by CV until stable current (overlay CVs) vs. potential achieved, and finally dried with argon.

The FDMA modified GC electrodes were then incubated in an aqueous solution of sulfo-NHS–biotin (1 mg mL^{-1}) in PBS overnight at 4 °C to attach biotin to the free terminal amines on the surface bound FDMA. The biotinylated electrodes were rinsed with copious amounts of Milli-Q™ water, scanned by CV until stable current vs. potential achieved, and finally dried with argon. At this point, construction of the affinity surfaces for the biospecific recognition of monoclonal anti-biotin IgG antibody was accomplished.

2.4. Anti-biotin IgG antibody complexation and immuno-biosensing interface refreshing via the displacement assay with free biotin

To prepare the final sensing interface, biotin modified electrodes were incubated in the aliquots of monoclonal anti-biotin IgG antibody (80 μL, 0.5 μg mL^{-1} in PBS, pH 7.4) for 30 min at room temperature. After the protein complexation, the electrode surface was rinsed with copious amounts of Milli-Q™ water to remove excess weakly bound protein. For the displacement assay, the anti-biotin IgG antibody bound electrode was exposed to 0.3 mg mL^{-1} free biotin solution in PBS, pH 7.4 for 20 min at room temperature. SWV measurements were recorded for this particular step at 0, 2, 5, 10, 15, and 20 min, respectively, to monitor the dissociation of the antibody from the surface bound epitope.

2.5. Step-wise fabrication surface characterization via X-ray photoelectron spectroscopy (XPS)

XPS data were acquired using an ESCALAB 220iXL spectrometer with a monochromatic $Al_{K\alpha}$ source (1486.6 eV), hemispherical analyzer and multichannel detector. Spectra were recorded in normal emission with the analyzing chamber operating below 10^{-9} mbar and selecting a spot size of approximately 1 mm^2. The incidence angle was set to 58° to the analyzer lens. The resolution of the spectrometer was about 0.6 eV as measured from the Ag $3d_{5/2}$ signal (full width at half maximum, fwhm) with a 20 eV pass energy. Survey scans were conducted between 1100 eV and 0 eV with a 1.0 eV step size, a 100 ms dwell time, and analyzer pass energy of 100 eV. High-resolution scans were run with 0.1 eV step size, dwell time of 100 ms and the analyzer pass energy set to 20 eV. All energies were reported as binding energies in eV and referenced to the C 1s signal (corrected to 285.0 eV). The XPS spectrum was analyzed with the curve-fitting program XPSPEAK4.1 and involved background subtraction using Shirley routine and a subsequent non-linear least-squares fitting to mixed Gaussian–Lorentzian functions (with Gaussian–Lorentzian ratio of C 1s 80%, N 1s 100%, Fe 2p 100% and S 2p 30%).

3. Results and discussion

3.1. XPS characterization of step-wise fabrication on GC surface

The step-wise fabrication of the immuno-biosensing interface on the GC surface was confirmed by XPS. The wide scan of biotin modified GC surfaces is shown in SI: Fig. 1a The XPS survey spectrum of immuno-biosensing interface (Fig. 1: Sensor 1 without antibody) showed the presence of an N 1s peak at about 399.7 eV (Ortiz et al., 1998) (amine, $–NH_2$) and 402.1 eV (Geneste et al., 2005) (hydroxylamine, –NHOH) were taken as an indication of MW being successfully grafted onto the GC (SI: Fig. 1b). This amine peak was believed to be a result of the aromatic $–NO_2$ at the meta position of the middle ring of the MW (which was not observed at 406 eV), being reduced to an $–NH_2$ (399.7 eV) or –NHOH (402.1 eV) during the electrochemical reduction of the aryl diazonium cations (Delamar et al., 1997). On GC, a potential of −0.6 V was considered strong enough to reduce the aromatic $–NO_2$ to $–NH_2$ and its derivatives including –NHOH (Jung et al., 1991; Louault et al., 2008; Mascarenhas et al., 2007). The absence of an N 1s peak at 403.8 eV and 405.1 eV confirmed that unreacted diazonium cations were not present on the surface (Combellas et al., 2005; Laforgue et al., 2005). Emissions from the C 1s core levels were deconvoluted into three functions: 1) C═C centered at 285.0 eV; 2) C–C and C–OH peak at approximately 286.5 eV; and 3) C═O emission at 288.9 eV (SI: Fig. 1c). Together the C 1s and N 1s XPS spectral data indicated that the mixed layer of MW/OEG 1:50 had been successfully attached onto the transducer surface.

Covalent attachment of the FDMA 1:50 MW/OEG derivatized surfaces was confirmed by the presence of nitrogen and iron emissions in the survey spectra. The high-resolution XPS scan of the Fe 2p region showed the two major spin–orbit components Fe $2p_{3/2}$ and Fe $2p_{1/2}$ at 708.6 eV and 721.2 eV, respectively, thus suggesting a major Fe(II) population with no evidence of Fe(III) species (SI: Fig. 1d). The best fit to the experimental N 1s signal was obtained with a linear combination of three Gaussian functions with binding energies of 399.3 eV ($–NH_2$), 400.4 eV (–NH) and 402.1 eV (–NHOH). Signals from both the free $–NH_2$ of the FDMA, and the reduced form of $–NO_2$ from MW to $–NH_2$, were suggested to contribute to the 399.3 eV peak. The peak at 400.4 eV was attributed to amide nitrogen atoms and finally 402.1 eV was attributed to –NHOH (reduced intermediate species of $–NO_2$ from MW) (SI: Fig. 1e). XPS data

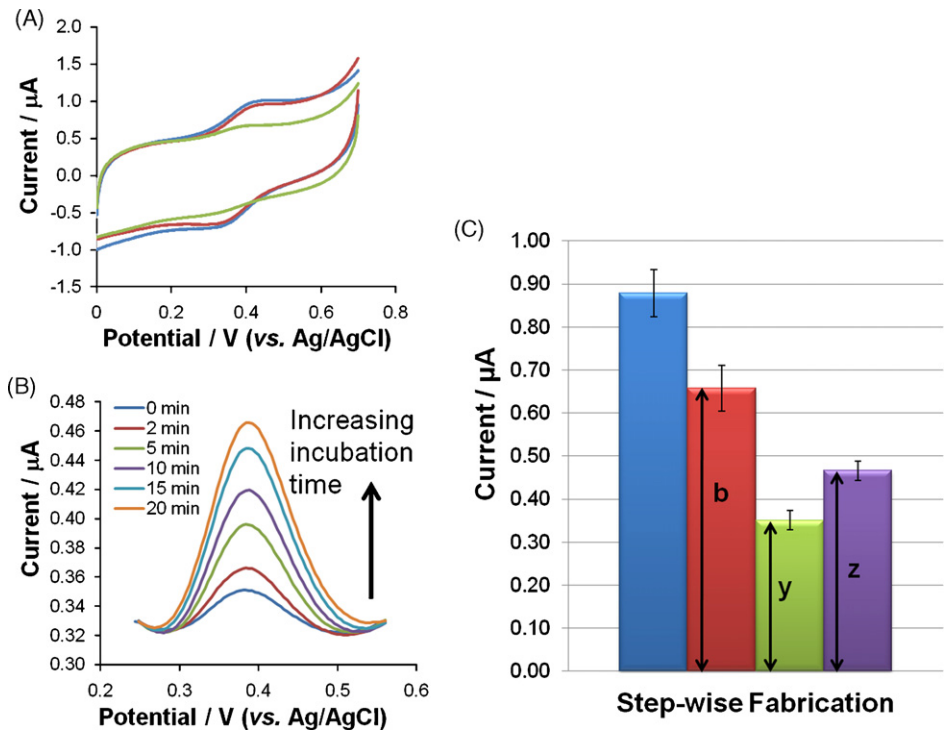

Fig. 2. (A) Electrochemical characterization of step-wise electrode surface modification via CV in 50 mM phosphate buffer, pH 7 (scan rate 100 mV s^{-1}); (B) response of the immuno-biosensor to free biotin via a displacement assay against incubation time using SWV in 50 mM phosphate buffer, pH 7; (C) representative bar chart showing the type of variation in current during each step in fabricating and using the biosensor. The formulas used for different binding events are (i) % attenuation = $(b-y)/b \times 100$ (epitope–antibody complexation); (ii) % increase = $(z-y)/y \times 100$ (the displacement assay). Note for lines and bars: FDMA (blue); biotin epitope (red); anti-biotin IgG (green) and free biotin (purple). The GC electrode is modified with MW/OEG 1:50. (For interpretation of the references to color in this figure legend, the reader is referred to the web version of the article.)

acquired for the N 1s regions before and after the attachment of FDMA suggested that there was no non-specific adsorption of FDMA onto the surface.

The attachment of biotin onto FDMA was confirmed by S 2p peak at 164.0 eV (SI: Fig. 1f). In the N 1s narrow scan, the dominant peak fitted at 400.2 eV was assigned to –NH contributed from amide bond between MW–FDMA, FDMA–biotin, and the biotin molecule itself. The smaller peaks at 399.3 eV ($-NH_2$) and 402.1 eV (–NHOH) were attributed to the reduction species of $-NO_2$ from MW (SI: Fig. 1g). Most importantly, with regard to the step-wise fabrication of the immuno-biosensing interface, a typical XPS N 1s narrow scan for each single step of the interface fabrication shows a high degree of amide bonds formed which is indicative of successful fabrication of the immuno-biosensing interface (mixed layer of MW/OEG–FDMA–biotin).

3.2. Electrochemical characterization of step-wise fabrication on GC surface

Fig. 2A illustrates the changes of CVs upon each step of surface modification. The electrode is first modified with MW/OEG 1:50, upon covalent attachment of FDMA, and then after the attachment of biotin to the FDMA, exhibits pronounced ferrocene electrochemistry. The exposure of the immuno-biosensing interface to anti-biotin IgG antibody solution causes an attenuation of this electrochemistry. Exposing the anti-biotin complexed immuno-biosensing interface to a sample which contains free biotin establishes a competition for the surface bound antibody. A consequence of this competition is that a portion of the antibodies dissociate from the surface bound epitope and complex with the free biotin in solution. An increase in the electrochemical signal via a displacement assay is then observed. Such an increase in current is illustrated in Fig. 2B where over a period of 20 min the peak current increased by 115 nA. For data analysis and interpretation, Fig. 2C shows the current measured by SWV for each single step of surface modification. It is important to note that due to the high affinity of the anti-biotin IgG for the surface bound biotin, not all the anti-biotin antibodies leave the epitope and the peak current was observed to rise to only 71% of the peak current recorded prior to complexing the antibody onto the electrode surface. Fig. 2C also shows the terminology used henceforth in relation to signal changes. The percentage attenuation is defined as the current after complexation of the antibody onto the surface divided by the current prior to antibody complexation (i.e., $(b-y)/b \times 100$ as shown in the figure). The percentage increase in current after the displacement assay is $(z-y)/y \times 100$.

3.3. The influence of the MW/OEG ratio on the biosensor performance

The molar ratio of MW to OEG influences the number of binding sites for FDMA, and hence epitope (biotin). This is evident in the electrochemical data presented in Fig. 3A where the FDMA current decreases as the ratio of MW/OEG decreases. The ratios presented in Fig. 3, and from here on, refer to the ratio of the two components in solution during the formation of the biosensing interface. Note that the extent of decrease in current at each electrode surface does not linearly follow the ratio of the two components in solution. That is the FDMA current observed does not decrease as significantly as the change in the ratio of MW/OEG in solution (Table 1), which indicates that the coverage of MW on the surface is greater than its ratio in solution. The MW, being the dominant surface species on the electrode surface, is consistent with the MW having a lower potential for reductive adsorption compared with the OEG (−417 mV and −864 mV, respectively) as reported previously (Liu et al., 2010; Louault et al., 2008).

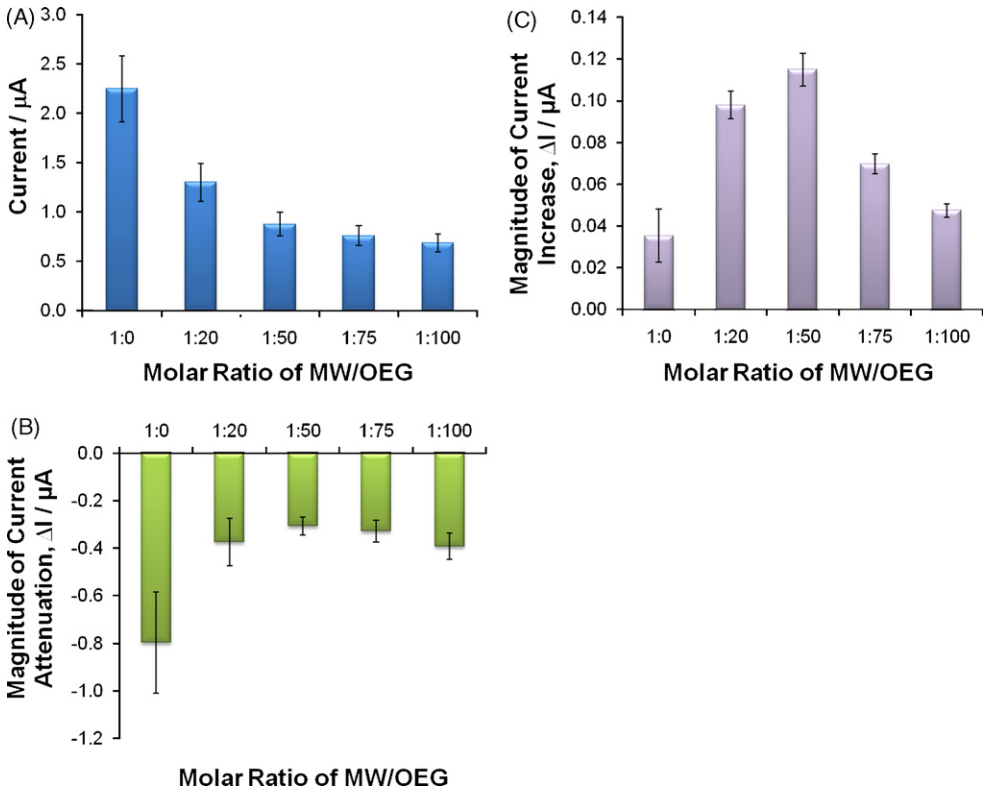

Fig. 3. The comparison of current signals obtained via SWV measurements in 50 mM phosphate buffer, pH 7: (A) after the attachment of FDMA; (B) the magnitude of current attenuation after exposure to anti-biotin solution; (C) the magnitude of current increase via a displacement assay at different molar ratios of MW/OEG.

The FDMA electrochemistry with an apparent formal potential of 349 mV (vs. Ag/AgCl) can allow the quantification of the number of ferrocene species on the electrode surface. As can be seen from Table 1 (see SI for calculation of the amount of FDMA on each electrode surface), a change from MW/OEG 1:0 to 1:100 sees a decrease in FDMA attached of only a third. Therefore, at the lowest ratio of MW/OEG, the area for each FDMA molecule (assuming homogeneous distribution) is 3.72 nm^2 (Table 1). A typical coupling yield for succinimide esters to primary amines is ~50% (Caprioara et al., 2007; Yang et al., 1999). Therefore, one can tentatively estimate the upper limit of the amount of sulfo-NHS–biotin that couples to the FDMA to give surface bound biotin as half the coverage of FDMA. Such a tentative estimate would suggest the area per surface bound epitope for antibodies to complex is about 7.44 nm^2 for the lowest ratio of MW/OEG. Based on the complete crystallographic dimensions of an IgG antibody reported was A_{front} = 85.1 nm^2, A_{side} = 65.8 nm^2, A_{top} = 57.9 nm^2 (Boehm et al., 1999; Pease Leonard et al., 2008), and each binding domain of an IgG antibody has dimensions of approximately 4 nm × 2.5 nm × 2.5 nm (Alzari et al., 1988; Stanfield et al., 1990), this density of surface epitopes provides sufficient space for an antibody to bind to each surface epitope, if they are homogeneously distributed across the surface.

The biotinylated interfaces were exposed to the 0.5 μg mL^{-1} monoclonal anti-biotin IgG antibody solution and the extent of current attenuation as a function of the molar ratio of MW/OEG is shown in Fig. 3B. The magnitude of the attenuation in current decreases from the MW/OEG 1:0 interface −0.80 μA (s = 0.21 μA, n = 5) to the 1:50 interface −0.31 μA (s = 0.04 μA, n = 5) whereupon, with more dilute surfaces the magnitude of the current attenuation increases once again. The initial decrease in current attenuation can be attributed to a lower amount of FDMA immobilized as there are fewer binding sites. Note that at high surface coverage of epitope there is significant steric hindrance for antibody to bind to the surface. Furthermore, there is less OEG layer to prevent the non-specific adsorption of IgG antibodies to the surface. As non-specific protein adsorption can also cause attenuation of the current, a significant proportion of the attenuation can be attributed to the non-specific protein adsorption. At interfaces of MW/OEG of 1:50 and lower, the estimated density of surface epitopes is sufficient for the antibody to bind to the surface. Furthermore, there is significant amount of OEG to limit the non-specific adsorption of antibodies and other proteins. Hence, at these ratios, the attenuation of the FDMA electrochemistry is attributed to mostly specific binding of the IgG antibodies to the surface epitope. The greater change in current at MW/OEG of 1:100 compared with the 1:50 can be attributed

Table 1
The quantification of the area per FDMA and the area per surface bound biotin.

Molar ratio of MW/OEG in solution	Q_{FDMA}	Γ_{FDMA} (mol/cm^2)	FDMA (molecules/cm^2)	Area per FDMA (nm^2)	Area per surface bound biotin (nm^2)
1:0	9.88E−07	1.46E−10	8.81E+13	1.14	2.28
1:20	5.71E−07	8.46E−11	5.09E+13	1.97	3.94
1:50	3.86E−07	5.71E−11	3.44E+13	2.91	5.82
1:75	3.34E−07	4.95E−11	2.98E+13	3.36	6.72
1:100	3.02E−07	4.47E−11	2.69E+13	3.72	7.44

to the antibody binding to the immuno-biosensing interface being more favourable (Fig. 3B and Table 1), possibly due to lower steric repulsion from neighboring antibodies (Rabbany et al., 1994).

The sensitivity of the sensor for free biotin detection is clearly influenced by the extent of attenuation of the ferrocene current. This is because this change represents the maximum amount the current can increase due to displacement of the surface bound antibodies by the target analyte in solution. However, the defining parameter for the analytical sensitivity is the amount of antibody that is displaced from the interface. As shown in Fig. 3C, the MW/OEG 1:50 shows the highest increase in current for the displacement assay compared to the other four interfaces evaluated. This interface happens to coincide with the interface with the lowest amount of current attenuation. Note, at high ratios of MW/OEG (1:0 and 1:20) there appears to be little increase in current signals. This is presumably because the majority of current attenuation is due to the non-specifically adsorbed antibody to the interface, and hence the biorecognition of antibody for the surface bound epitope is not involved. As the displacement assay requires the competition for antibody binding sites between surface bound epitope and target analyte in solution, non-specifically adsorbed antibody will not be displaced. At the lowest epitope densities (1:75 and 1:100) presumably the antibody is more strongly bound to the surface epitope (no repulsion effect of antibody density) and hence also is not displaced. Thus it seems that the interface with the ratio of MW/OEG of 1:50 is the best compromise between having the antibody specifically adsorbed but not too strongly bound to the interface, and will be used henceforth. This does suggest the surface epitope being of lower affinity for the antibodies than the analyte will facilitate higher displacement assay sensitivity.

3.4. Immuno-biosensor reproducibility

The reproducibility of the immuno-biosensor, fabricated with the optimal MW/OEG 1:50 molar ratio in solution, when exposed to free biotin (0.3 mg mL^{-1}), was assessed using 5 electrodes prepared in the same manner. As shown in SI: Fig. 2, the relative standard deviation (RSD) achieved was 6.8% (mean current = 0.1108 μA, s = 0.0075 μA, n = 5). This result was considered good in terms of immuno-biosensor sensitivity (Giroud et al., 2009) towards concentration dependence of detecting small target analyte especially for a displacement assay. Furthermore, this result was also in line with the observation that molar ratio of MW/OEG 1:50 (Fig. 3) gave the best balance between specific epitope–antibody complexation and the extent of displacement of bound antibody by free biotin.

3.5. Immuno-biosensor repeatability

The repeatability of the immuno-biosensor was next investigated where the sensor was first exposed to the anti-biotin IgG antibody solution followed by free biotin solution to displace bound antibody. Subsequently, the biorecognition interface was refreshed by holding the potential to −800 mV for 10 min (vs. Ag/AgCl) to remove as much surface bound antibody as possible. The original electrode was reincubated into the antibody solution such that the antibody could again bind with the epitope and the displacement assay could again be performed. This was conducted ten times within 24 h. The antibody–antigen binding was found to be reversible, and is consistent with previous studies (Cash et al., 2009; Giroud et al., 2009). The displacement assay shows little variation of electrochemical signal after ten repeated measurements, RSD 9.6% (mean current = 0.1498 μA, s = 0.0143 μA, n = 10) (SI: Fig. 3).

This repeatability study has also successfully demonstrated the capability of a single immuno-biosensing interface to be used multiple times for successive big molecule (monoclonal anti-biotin IgG antibody) and small organic molecule (free biotin) detection. This was an encouraging result as this demonstrated the interface provides a robust platform for immuno-biosensing applications.

4. Conclusions

In conclusion, here it is shown that the sensor interfacial design is crucial to sensor performance for the immuno-biosensor described for the detection of small molecules. The XPS, CV, and SWV results confirmed the successful step-wise fabrication of the immuno-biosensing interface. Each component was covalently attached to the immuno-biosensing interface to form a label-free immuno-biosensor. The fabricated immuno-biosensor showed good reproducibility (RSD 6.8%) and repeatability (RSD 9.6%) if a short cathodic polarization at −800 mV for 10 min was used to refresh the sensing interface. A logical extension of this work is to apply this optimized condition to real analyte detection. Preliminary studies show the prototype system can be used for drug detection in complex matrices.

Acknowledgements

The authors gratefully thank Muthukumar Chockalingham and Dr. Erwann Luais for technical assistance on running XPS, and Dr. Joshua Peterson for useful comments on this manuscript. This research was supported under the Australian Research Council Linkage projects funding scheme (LP0775216) and Sook Mei Khor would like to thank the Malaysian government, The Ministry of Higher Education and University of Malaya, Malaysia for the award of an SLAI scholarship.

Appendix A. Supplementary data

Supplementary data associated with this article can be found, in the online version, at doi:10.1016/j.bios.2010.08.082.

References

Alzari, P.M., Lascombe, M.B., Poljak, R.J., 1988. Annu. Rev. Immunol. 6, 555–580.
Bahr, J.L., Yang, J., Kosynkin, D.V., Bronikowski, M.J., Smalley, R.E., Tour, J.M., 2001. J. Am. Chem. Soc. 123, 6536–6542.
Baranton, S., Belanger, D., 2005. J. Phys. Chem. B 109, 24401–24410.
Boehm, M.K., Woof, J.M., Kerr, M.A., Perkins, S.J., 1999. J. Mol. Biol. 286, 1421–1447.
Bonanno, L.M., DeLouise, L.A., 2010. Anal. Chem. 82, 714–722.
Caprioara, M., Fiammengo, R., Engeser, M., Jaeschke, A., 2007. Chem. Eur. J. 13, 2089–2095.
Cash, K.J., Ricci, F., Plaxco, K.W., 2009. Chem. Commun. 41, 6222–6224.
Combellas, C., Delamar, M., Kanoufi, F., Pinson, J., Podvorica, F.I., 2005. Chem. Mater. 17, 3968–3975.
Creager, S., Yu, C.J., Bamdad, C., O'Connor, S., MacLean, T., Lam, E., Chong, Y., Olsen, G.T., Luo, J., Gozin, M., Kayyem, J.F., 1999. J. Am. Chem. Soc. 121, 1059–1064.
Delamar, M., Desarmot, G., Fagebaume, O., Hitmi, R., Pinson, J., Saveant, J.M., 1997. Carbon 35, 801–807.
Fan, F.-R.F., Yang, J., Dirk, S.M., Price, D.W., Kosynkin, D., Tour, J.M., Bard, A.J., 2001. J. Am. Chem. Soc. 123, 2454–2455.
Geneste, F., Moinet, C., Ababou-Girard, S., Solal, F., 2005. New J. Chem. 29, 1520–1526.
Giroud, F., Gorgy, K., Gondran, C., Cosnier, S., Pinacho, D.G., Marco, M.P., Sanchez-Baeza, F.J., 2009. Anal. Chem. 81, 8405–8409.
Gooding, J.J., 2008. Electroanalysis 20, 573–582.
Guo, Y., Ye Jing, Y., Divin, C., Huang, B., Thomas Thommey, P., Baker James Jr., R., Norris Theodore, B., 2010. Anal. Chem. 82, 5211–5218.
Jung, H., Shaikh, A.U., Heflich, R.H., Fu, P.P., 1991. Environ. Mol. Mutagen. 17, 169–180.
Laforgue, A., Addou, T., Belanger, D., 2005. Langmuir 21, 6855–6865.
Leckband, D., Sheth, S., Halperin, A., 1999. J. Biomater. Sci. Polym. Ed. 10, 1125–1147.
Liu, G., Boecking, T., Gooding, J.J., 2007a. J. Electroanal. Chem. 600, 335–344.
Liu, G., Paddon-Row, M.N., Gooding, J.J., 2007b. Electrochem. Commun. 9, 2218–2223.
Liu, G., Chockalingham, M., Khor, S.M., Gui, A.L., Gooding, J.J., 2010. Electroanalysis 22, 918–926.
Liu, G., Gooding, J.J., 2006. Langmuir 22, 7421–7430.
Liu, G., Liu, J., Boecking, T., Eggers, P.K., Gooding, J.J., 2005. Chem. Phys. 319, 136–146.
Liu, G., Paddon-Row, M.N., Gooding, J.J., 2008. Chem. Commun. 33, 3870–3872.
Louault, C., D'Amours, M., Belanger, D., 2008. Chem. Phys. Chem. 9, 1164–1170.

Mascarenhas, R.J., Namboothiri, I.N., Sherigara, B.S., Mahadevan, K.M., 2007. Croat. Chem. Acta 80, 53–59.
McPherson, T., Kidane, A., Szleifer, I., Park, K., 1998. Langmuir 14, 176–186.
Ortiz, B., Saby, C., Champagne, G.Y., Belanger, D., 1998. J. Electroanal. Chem. 455, 75–81.
Ossola, F., Tomasin, P., Benetollo, F., Foresti, E., Vigato, P.A., 2003. Inorg. Chim. Acta 353, 292–300.
Pease Leonard 3rd, F., Elliott John, T., Tsai, D.-H., Zachariah Michael, R., Tarlov Michael, J., 2008. Biotechnol. Bioeng. 101, 1214–1222.
Rabbany, S.Y., Kusterbeck, A.W., Bredehorst, R., Ligler, F.S., 1994. J. Immunol. Methods 168, 227–234.
Stanfield, R.L., Fieser, T.M., Lerner, R.A., Wilson, I.A., 1990. Science 248, 712–719.
Tour, J.M., Rawlett, A.M., Kozaki, M., Yao, Y., Jagessar, R.C., Dirk, S.M., Price, D.W., Reed, M.A., Zhou, C.W., Chen, J., Wang, W., Campbell, I., 2001. Chem. Eur. J. 7, 5118–5134.
Viljas, J.K., Pauly, F., Cuevas, J.C., 2008. Phys. Rev. B: Condens. Matter Mater. Phys. 77, 155119/155111–155119/155114.
Yang, D.J., Ilgan, S., Higuchi, T., Zareneyrizi, F., Oh, C.-S., Liu, C.-W., Kim, E.E., Podoloff, D.A., 1999. Pharm. Res. 16, 743–750.
Zanini, S., Mueller, M., Riccardi, C., Orlandi, M., 2007. Plasma Chem. Plasma Process. 27, 446–457.